

**STRUCTURAL AND MORPHOLOGICAL STUDIES OF Ce DOPED HYDROXYAPATITE SYNTHESIZED BY SOLGEL METHOD****S.Saranya & M.Prema Rani\****\*Research Centre PG Department of Physics, the Madura College, Madurai-11, Tamilnadu, India.***(Received on Date: 1 August 2019****Date of Acceptance: 7 September 2019)****ABSTRACT**

The present work reports a simple adapted Sol gel method for the synthesis of Ce substituted Ca hydroxyapatite (HAp). The structural and morphological properties of the Ce-doped hydroxyapatite (Ce-HAp) were characterized by X-ray diffraction (XRD), scanning electron microscopy (SEM) and energy dispersive X-ray analysis (EDAX). Undoped hydroxyapatite (HAp) and Ce substituted HAp samples with variable amounts (0.07, 0.15, 0.22) % of Ce were synthesized by sol-gel method. The results of the XRD studies revealed the progressive increase in the crystallite size from 21 to 24nm with increasing Ce concentration. The FTIR spectra proved formation of HAp due to the presence of hydroxyl and phosphate functional groups in all samples.

**No: of Tables: 04****No: of Figures: 25****No: of References: 17**

## INTRODUCTION

Hydroxyapatite is chemically similar to the mineral component of bones and hard tissues in mammals. It is one of few materials that are classed as bioactive, meaning that it will support bone in growth and osseointegration when used in orthopaedic, dental and maxillofacial applications. It has the ability to integrate in bone structures and support bone in growth, without breaking down or dissolving (i.e. it is bioactive) [1]. Hydroxyapatite is a thermally unstable compound, decomposing at temperature from about 800-1200°C depending on its stoichiometry. Coatings of hydroxyapatite are often applied to metallic implants to alter the surface properties. In this manner the body sees hydroxyapatite type material which it is happy to accept. Hydroxyapatite may be employed in forms such as powders, porous blocks or beads to fill bone defects or voids [2]. These may arise when large sections of bone have had to be removed (e.g. bone cancers) or when bone augmentations are required (e.g. maxillofacial reconstructions or dental applications).

Hydroxyapatite based ceramics have been evaluated for a variety of applications in spinal surgery, utilizing in vivo animal models and human clinical series. As an osteoconductive material, it appears to function best as a bone graft

extender or carrier for an osteoinductive bone growth factor rather than as a stand-alone bone graft substitute in nonstructural clinical applications. Cerium has no known biological role in humans, but is not very toxic either; it does not accumulate in the food chain to any appreciable extent [3]. Because it often occurs together with calcium in phosphate minerals, and bones are primarily calcium phosphate, cerium can accumulate in bones in small amounts that are not considered dangerous. Cerium, like the other lanthanides, is known to affect human metabolism, lowering cholesterol levels, blood pressure, appetite, and risk of blood coagulation.

A large number of studies were also conducted in order to discover new biomaterials with improved biological and physicochemical properties (especially antibacterial and luminescent) in order to be successfully used in the biomedical field [4].

As Ce cations possess luminescent properties (under UV excitation) and antimicrobial activity, their incorporation in the structure of HAp could lead to a biomaterial being obtained with promising applications in medicine (for imaging, drug delivery)

The aim of this work was also to study the influence of cerium on the Structural and Morphological studies of Hydroxyapatite doped with small concentrations of cerium.

## Experimental Procedure

### To obtain Pure HAP

A Stoichiometric amount of calcium nitrate tetra hydrate ( $\text{Ca}(\text{NO}_3)_2 \cdot 4\text{H}_2\text{O}$ ) and diammonium hydrogen phosphate was dissolved in distilled water. The solution was stirred in a magnetic stirrer for about 8 hours at  $90^\circ\text{C}$ .  $\text{pH}$  was maintained as 10 by adding ammonium hydroxide. After the formation of gel the sample was dried at  $110^\circ\text{C}$  for 22 hours. The dried samples were ground using mortar and pestle. The sample was sintered in the furnace at  $750^\circ\text{C}$  for 2 hrs. The final product formed was obtained as fine white powder.

### To Obtain Cerium doped HAP

Ce doped hydroxyapatite with different concentration [where  $x = 0.07\%$ ,  $0.15\%$ ,  $0.22\%$ ] of  $0.1\text{M}$  was synthesized by sol-gel method. Cerium doped hydroxyapatite was prepared by dissolving stoichiometric amount of calcium nitrate tetrahydrate, Cerium nitrate tetrahydrate are dissolved in a  $200\text{ml}$  beaker and taken as 'A' Solution. Diammonium hydrogen phosphate was

dissolved in distilled water in a separate beaker marked as 'B' Solution. The mixture of 'A' Solution was slowly added to the 'B' Solution. The mixture of sol was stirred vigorously on a magnetic stirrer for 8 hours for uniform mixing. The gel was heated at  $110^\circ\text{C}$  for 22 hours to obtain powder. The obtained powder of was then annealed at  $750^\circ\text{C}$  for 2hrs. Finally the white powder was obtained.

## RESULTS AND DISCUSSION

### X-ray diffraction (XRD)

X-ray powder diffraction measurements were performed at SAIF (Sophisticated Analytical Instrument Facility), Cochin using  $\text{CuK}\alpha_1$  with  $2\theta$  range from  $10^\circ$  to  $120^\circ$  and  $0.02^\circ$  step sizes. The XRD profiles of the pure hydroxyapatite and Cerium doped hydroxyapatite are given in figures 1.1a-1.1d respectivel. The combined XRD profile for for different samples shown in figure 1.1e. The broad peaks in the X-ray diffraction patterns assigned to the characteristic (002), (211), (213), (222), (112) planes of  $\text{Ca}_{10-x}\text{Ce}_x(\text{PO}_4)_6(\text{OH})_2$  were in accordance with the expected patterns for crystalline hydroxyapatite with a hexagonal structure (JCPDS No. 460905). The crystallite size was calculated from full-

width-at-half-maximum (FWHM) for the diffraction peaks. The crystallite size

calculated for the samples is shown in table1

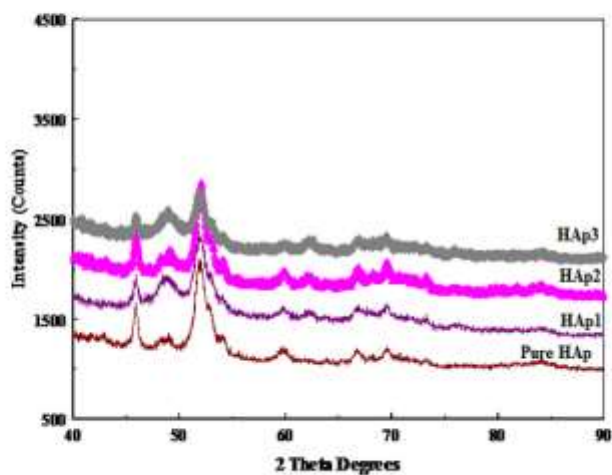


Fig 1 Combined xrd profile of Pure and Ce doped HAp

Table 1 Crystallite size of Hydroxyapatite and Ce doped Hydroxyapatite.

S.No.	Sample	Crystallite size (nm)
1	Pure HAp	21.56
2	HAp1	22.68
3	HAp2	24.31
4	HAp3	25.56

## FTIR ANALYSIS

FTIR of the samples were taken at International Research Centre, Kalasalingam University, Krishnankoil. The presence of functional groups was confirmed using Fourier transform infrared spectroscopy. The spectrum was recorded in the range 4000-400  $\text{cm}^{-1}$ . The resolution of spectrometer was 4  $\text{cm}^{-1}$ . FTIR spectra show all characteristic absorption peaks of HAp.

The peaks at 3565  $\text{cm}^{-1}$ , 3462  $\text{cm}^{-1}$  confirm the presence of hydroxyl group. The FTIR Spectrum for different samples are shown in the figure 1.2a- 1.2d. The intense broad peak at 875  $\text{cm}^{-1}$  confirms the presence of  $\text{PO}_4^{3-}$  in the samples. The shifts in the IR absorption bands of phosphate groups of the samples were observed and it decreases with increase in dopant concentration. The transmitted data of samples are in table 2

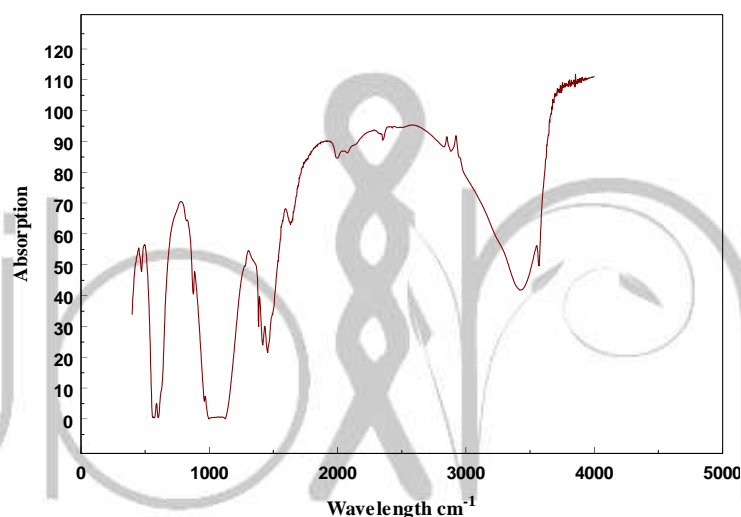
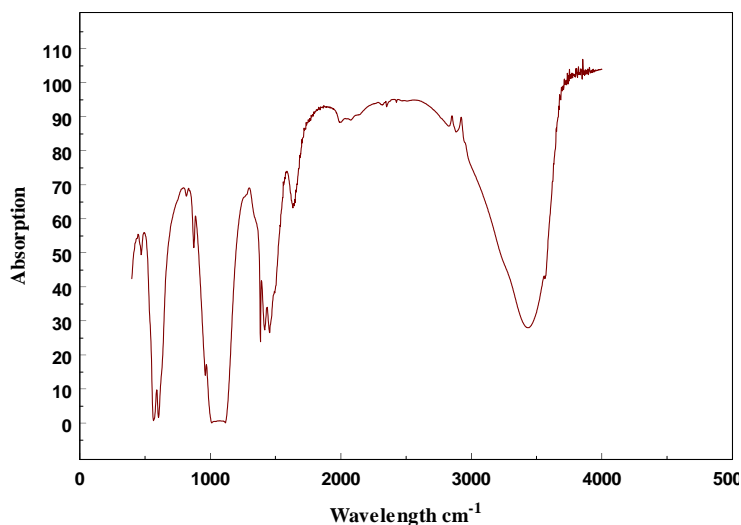
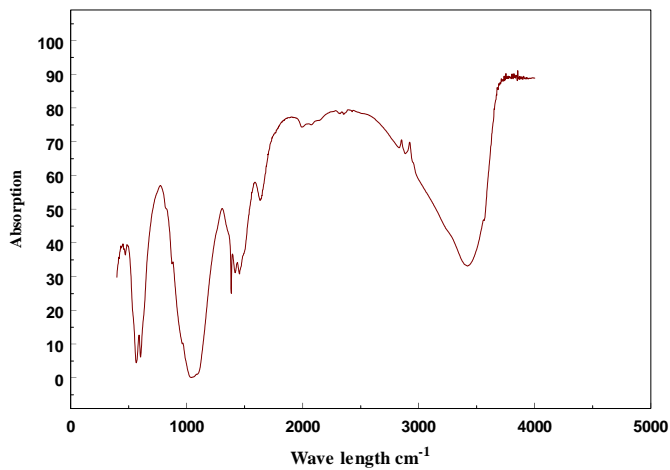


Fig 1.2a FTIR spectrum of pure HAp



**Fig 1.2b FTIR spectrum of 0.075% Ce doped HaP**



**Figure 1.2c FTIR spectrum of 0.15% Ce doped HaP**

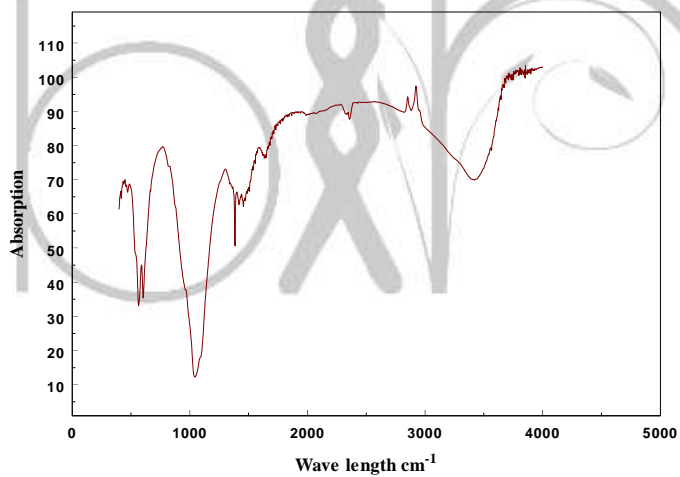


**Figure 1.2d FTIR spectrum of 0.22% Ce doped HaP**

**Table 2 Transmittance data of Synthesized HAp Samples**

Chemical group	Pure HAp	0.075% Ce doped HAp	0.15% Ce doped HAp	0.225% Ce doped HAp	comments
OH <sup>-</sup>	3570.24	3570.24	3570.24	3570.24	Presence of HAp Decreases with dopant concentration
	3423.65	3417.86	3514.93	-	
HPO <sub>4</sub> <sup>2-</sup>	601.79	603.72	603.72	603.72	Increases after doping HAp

### Scanning Electron Microscope (SEM)

SEM data was collected at Gandhigram University, Dindigul. SEM can achieve resolution better than 1 nanometer. The SEM images are shown in figures 1.3(a) – 1.3(d). Structural variations are observed for the Pure and Ce doped hydroxyapatite nanostructures. From SEM images, it could be observed that the

increase in the Ce concentration slightly influenced the morphology of the samples. As seen in the pictures, the morphology slightly varied with the addition of cerium. This might be due to the ionic substitutions in the crystal lattice to compensate the charge imbalance between Ce<sup>3+</sup> and Ca<sup>2+</sup> ions

**Fig 1.3a Pure HAp**



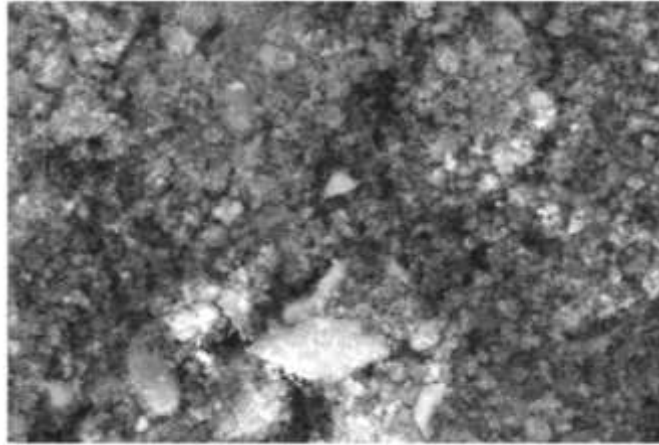


**Fig 1.3b 0.07% Ce doped HAp**

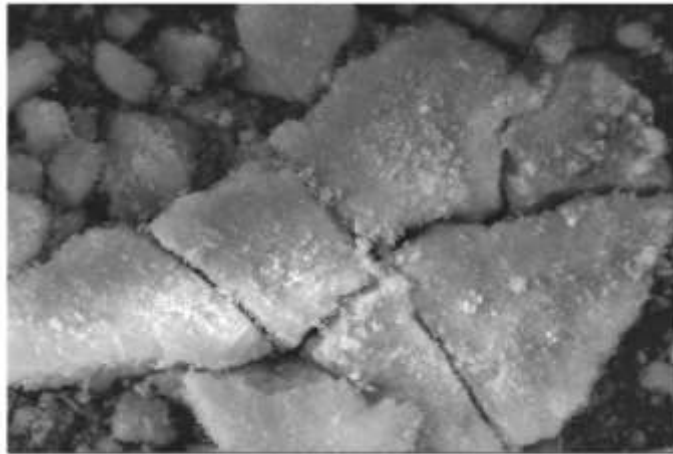


**Fig 1.3c 0.15% Ce doped HAp**

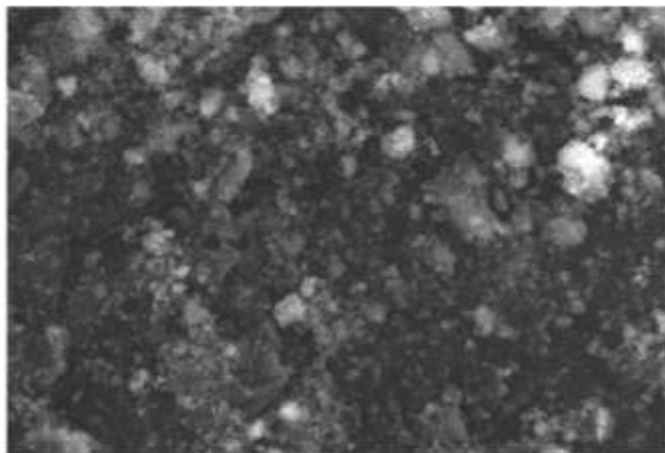


**Fig 1.3d 0.22 % Ce doped HAp**



**EMISSION DISPERSIVE SPECTROSCOPY**

The EDAX spectra studied powders confirmed the presence of all constituent elements of the Ce:HAp powders Ce, Ca, P and O. This is shown in figures 1.4(a) – 1.4 (d). These results suggest that cerium ions

were incorporated in the hydroxyapatite structure. Moreover, these studies confirmed the increase of the Ce concentrations in the samples. The composition of elements is given in table 3.

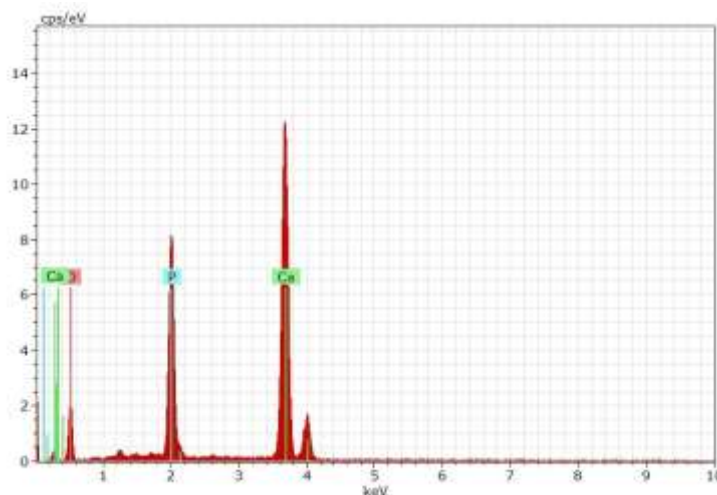


**Fig 1.4a. Pure HAp**

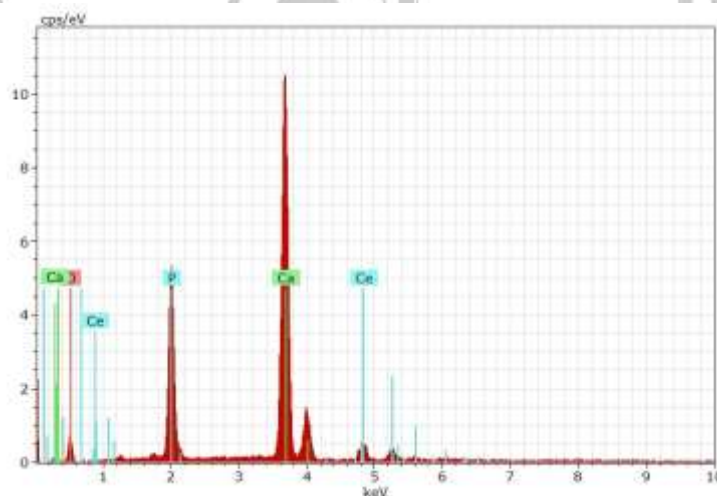


**Fig 1.4b. 0.07% Ce doped HAp**

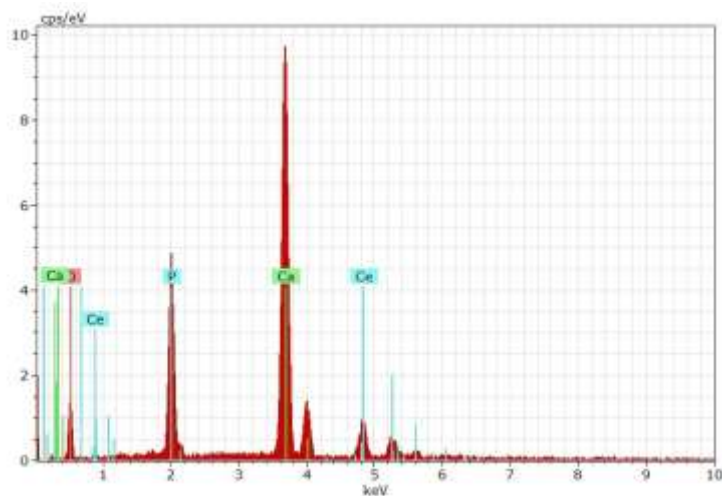


Fig 1.4c. 0.15% Ce doped HAp

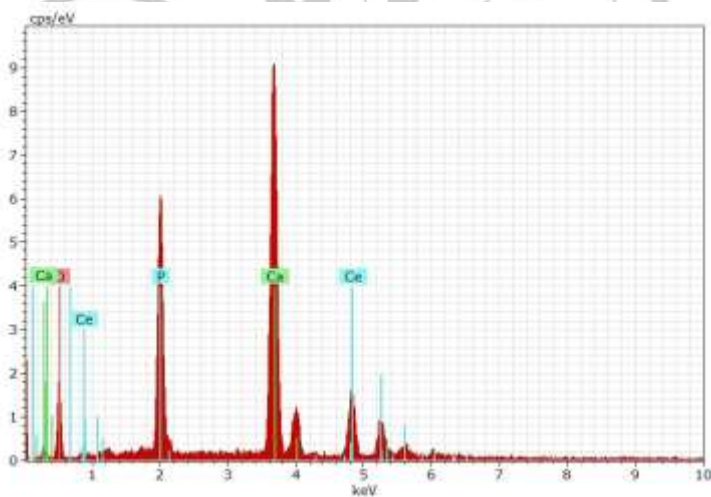


Fig 1.4 d. 0.22% Ce doped HAp

Table 3 Elemental compositions of HAp and Ce-HAp

Samples	Ca	P	O	Ce
Pure HAp	71.26	18.21	10.53	-
0.07% of Ce	31.71	14.73	51.87	1.69
0.15% of Ce	23.48	10.93	63.30	2.28
0.22% of Ce	21.10	13.99	61.38	3.54

### Differential Thermal Analysis:

This analysis has been done in SAIF, Cochin. From this technique we see that when the temperature increases the weight of the sample decreases. In DTA the material under study are made to undergo thermal cycles while recording the temperature difference between the sample and the reference material. From

this we say that the change in the sample is endothermic process. The Differential thermal Analysis for different samples are shown in figure 1.5a-1.5d. The obtained DTA curve revealed an intense endothermic peak at 310 °C with an associated weight loss in the range 300°C–200°C that was attributed to absorbed moisture

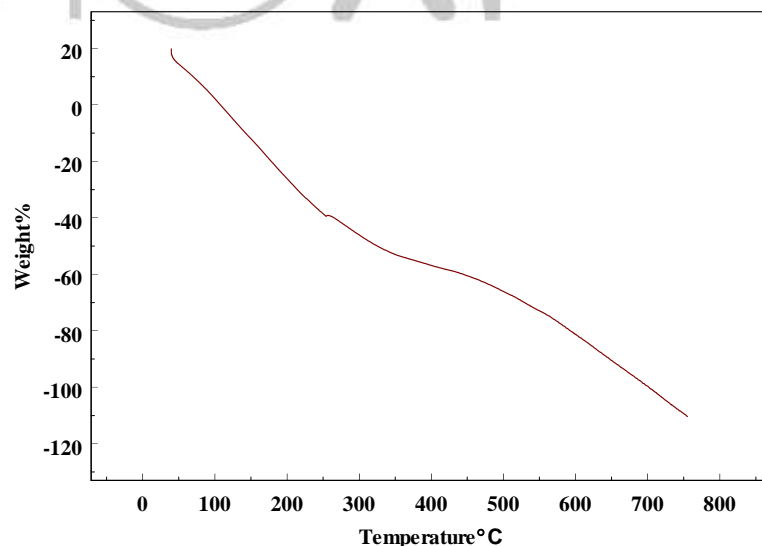
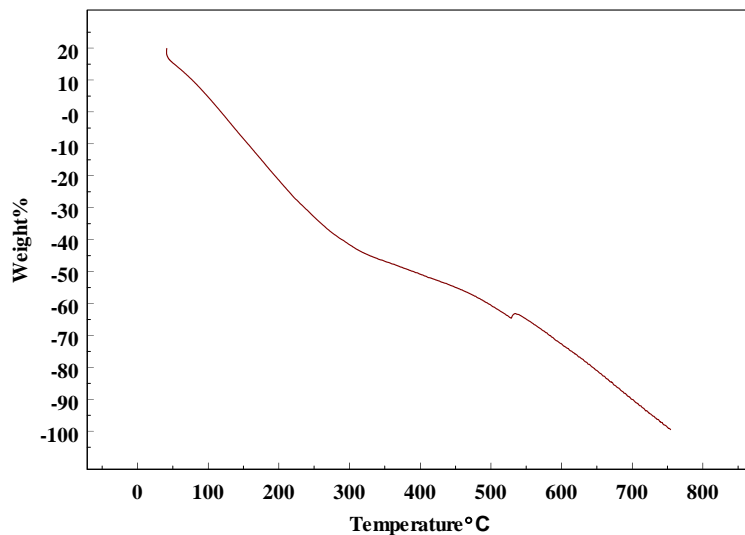
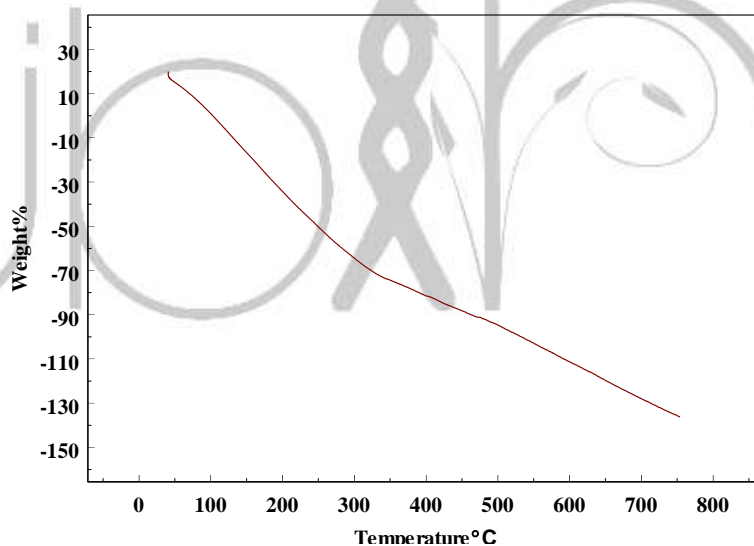


Fig 1.5a DTA Curve of Pure HAp



**Fig 1.5b DTA Curve of 0.07% Ce doped HAp**



**Fig 1.5c DTA Curve of 0.15% Ce doped HAp**

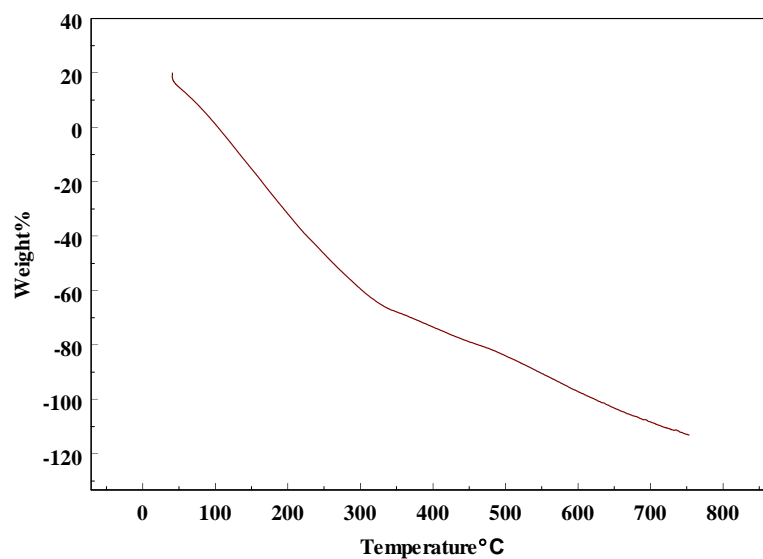


**Fig 1.5 d DTA Curve of 0.22% Ce doped HAp**

### **Thermal Gravimetric Analysis:**

This analysis has been done in SAIF, COCHIN. The thermal decomposition mechanism of the composite dried gels was studied by TGA measurements. In this technique as the temperature increases

the mass changed and the weight loss has been observed in the temperature ranges between 300°C to 400 °c. The total weight losses observed were in the temperatures range of 300°C- 750°C. The TGA graphs for different samples are shown in figure 1.6 a- 1.6 d.

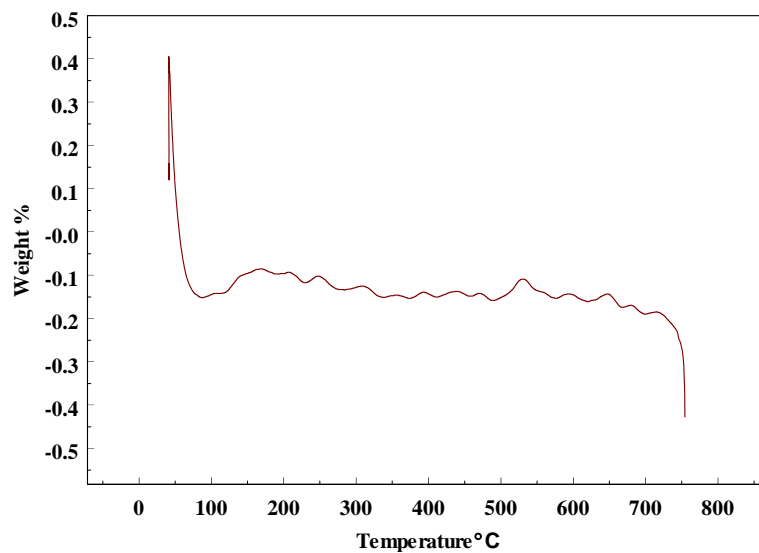


Fig 1.6 a TGA Curve of Pure HAp

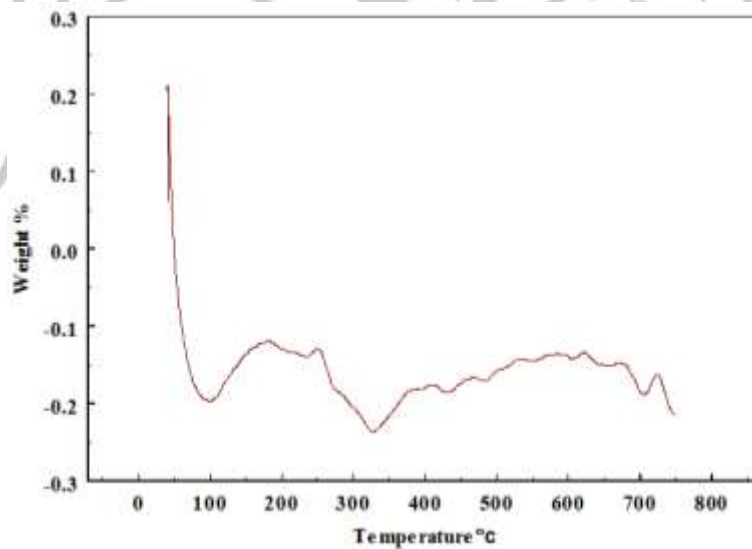


Fig 1.6 b TGA Curve of 0.07% Ce doped HAp

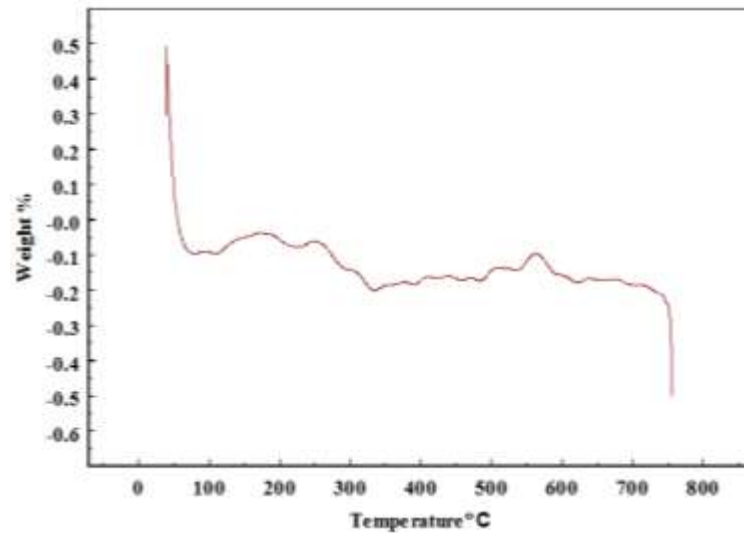


Fig 1.6 c TGA Curve of 0.15% Ce doped HAP

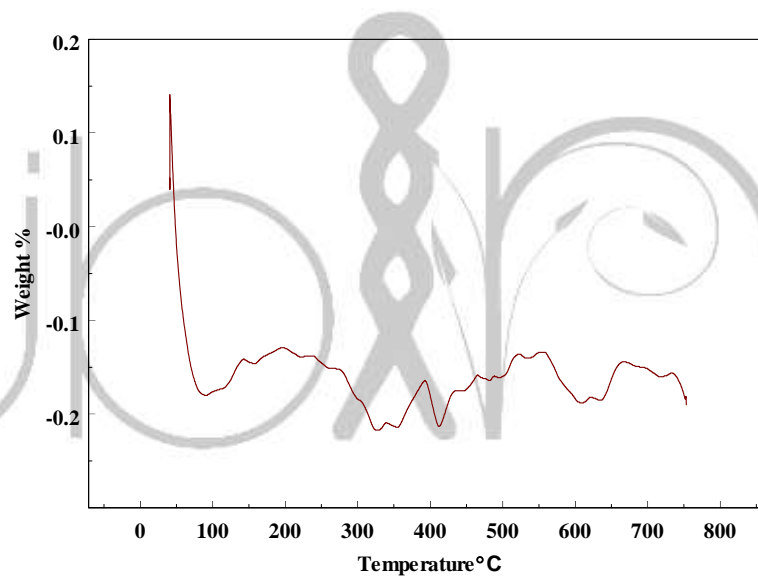


Fig 1.6 d TGA Curve of 0.22% Ce doped HAP

## ANTI MICROBIAL TEST

By using agar diffusion method anti microbial susceptibility testing was done at The Department of Biotechnology, The Madura College, and Madurai-11. Agar plates were inoculated with a standardized inoculum of the Escherchia coli. Then filter paper discs

(about 6mm in diameter), containing  $\text{Ca}_{10-x}\text{Ce}_x(\text{PO}_4)_6(\text{OH})_2$  where ( $x=0, 0.07\%, 0.15\%, 0.22\%$ ) were placed on the agar surface. The petri dishes were incubated under suitable conditions. Then samples were diffused into the agar the growth of the test microorganism in the samples was monitored. The and then the diameter of inhibition growth zones were measured



and tabulated in table. Thus cerium doped HAp had anti bacterial effect and it increases with increase in cerium concentration. The Antimicrobial activity

for different samples are shown in the figure 1.7a-1.7d. The diameter in inhibition of zone of different samples are shown in table



**Fig 1.7a Pure HAp**



**Fig 1.7b 0.07% Ce doped HAp**



**Fig 1.7c 0.15% Ce doped HAp**



**Fig 1.7d 0.22% Ce doped HAp**

**Table 4****Antimicrobial activity of the Cerium compound treated against *Eschericia coli***

S.No	Sample	Diameter of the inhibition zone in mm
1	Pure HAp	9
2	0.07 % Ce doped HAp	11
3	0.15 % Ce doped HAp	13
4	0.22% Ce doped HAp	14

**Conclusion**

Both Ce-free and Ce-containing HAp samples with high crystallinity and of high purity were successfully synthesized by the sol-gel method. The crystal size decreased with increasing concentration of Ce. The results obtained in the XRD studies demonstrated that the Ce-HAp powders synthesized by an adapted sol gel method gave hydroxyapatite with a good crystalline structure without any new phases or impurities. The crystallite size increases from the pure HAp which may be due to the larger ionic radius of Cerium compared with calcium. Doping of Ce causes structural changes which affect the crystalline nature of the sample. The surface morphology and elemental composition of the samples slightly changed with the addition of Ce, Thus, the trivalent Ce<sup>3+</sup> ions can substitute divalent Ca<sup>2+</sup> ions in HAp. EDX analysis indicates

the phase purity and crystallinity of the HAp powder. From EDX spectra the doped and undoped element composition is confirmed. FTIR confirmed that the HAp was synthesized by the presence of HPO<sub>4</sub> with the wave number in the order of 870cm<sup>-1</sup>. From DTA curve we obtained the weight of the sample. As the temperature increases the weight of the sample decreases. The change in the sample is endothermic process. From TGA curve, weight loss has been observed between the range 300°C to 400°C. Anti bacterial effect of cerium doped HAp was confirmed from anti bacterial susceptibility test.

**REFERENCES**

**J. Park**, Bioceramics: Properties, Characterizations, and Applications, Springer, New York, 2008. (359 pp.).

**S. Weiner, H.D. Wagner,** Material bone: structure-mechanical function relations, *Annu. Rev. Mater. Sci.* 28 (1998) 271–298.

**H. Pan, B.W. Darvell,** Effect of carbonate on hydroxyapatite solubility, *Crystal Growth Des.* 10 (2010) 845–850.

**K. Agrawal, G. Singh, D. Puri, S. Prakash,** Synthesis and characterization of hydroxyapatite powder by sol–gel method for biomedical application, *J. Miner. Mater. Charact. Eng.* 10 (2011) 727–734.

**M.A. Jakupec, P. Unfried, B.K. Keppler,** Pharmacological properties of cerium compounds, *Rev. Physiol. Biochem. Pharmacol.* 153 (2005) 101–111.

**Y. Lin, Z. Yang, J. Cheng,** Preparation, characterization and antibacterial property of Cerium substituted hydroxyapatite nanoparticles, *J. Rare Earths* 25 (2007) 452–456.

**Y. Huang, Y. Wang, C. Ning, K. Nan, Y. Han,** Preparation and properties of a cerium-containing hydroxyapatite coating on commercially pure titanium by micro-arc oxidation, *Rare Metals* 27 (2008) 257–260.

**K. Balani, R. Anderson, T. Laha, M. Andara, J. Tercero, E. Crumpler, A. Agarwal,** Plasma-sprayed carbon nanotube reinforced hydroxyapatite coatings and their interaction with human osteoblasts in vitro, *Biomaterials* 28 (2007) 618–624.

**Z. Feng, Y. Liao, M. Ye,** Synthesis and structure of cerium-substituted hydroxyapatite, *J. Mater. Sci. Mater. Med.* 16 (2005) 417–421.

**T. Ishikawa, H. Tanaka, A. Yasukawa, K. Kandori,** Modification of calcium hydroxyapatite using ethyl phosphates, *J. Mater. Chem.* 5 (1995) 1963–1967.

**V. Berezovskaya, N. P. Efrushina, E. V. Zubar, V. P. Dotsenko,** in Proceedings of the International Conference Nanomaterials: Applications and Properties, Sumy State University, Ukraine, 2012, Abstract No. 01PCN24

**Messing GL, Zhang SC, Jayanthi GV.** Ceramic powder synthesis by spray pyrolysis. *Journal of the American Ceramic Society* 1993;76(11):2707–26.

**Z. Feng, Y. Liao, M. Ye,** Synthesis and structure of cerium-substituted hydroxyapatite, *J. Mater. Sci. Mater. Med.* 16 (2005) 417–421.

**Z.F. Chena, B.W. Darvell, V.W.H. Leung,** Hydroxyapatite solubility in simple inorganic solutions, *Arch. Oral Biol.* 49 (2004) 359–367.

**Grandjean-Laquerriere A, Laquerriere P, Jallot E, Nedelec JM, Guenounou M, Laurent-Maquin D, Phillips TM** (2006) *Biomaterials* 27:3195

**M. Mazaheri, M. Haghightzadeh, A.M. Zahedi, S.K. Sadrnezhad,** Effect of a novel sintering process on mechanical properties

of hydroxyapatite ceramics, J. Alloys Compd. 471 (2009) 180–184.

**Y.M. Sung, Y.K. Shin, J.J. Ryu**, Preparation of hydroxyapatite zirconia bioceramic nanocomposites for orthopedic and dental prosthesis application, Nanotechnology 18 (2007) 065602.

